# A Radiation Hardened CMOS Image Sensor with Almost Zero Dark Current Increase During Radiation

Takashi Watanabe [1], Tomoaki Takeuchi [2], Osamu Ozawa [3], Hirohisa Komanome [3], Tomoyuki Akahori [1], Kunihiko Tsuchiya [2]

[1] Brookman Technology, Inc. 125 Daikumachi, Naka-ku, Hamamatsu, Shizuoka, 430-0936, Japan
Tel : +81-53-482-7741, Fax : +81-53-482-7742, E-mail : twata@brookmantech.com

[2] Japan Atomic Energy Agency, 4002 Narita, Oarai, Higashiibaraki, Ibaraki 311-1393, Japan

[3] Ikegami Tsushinki Co., Ltd, 3-6-16 Ikegami, Ohta-ku, Tokyo, 146-8567, Japan

***Abstract* – Radiation hard image sensors have been developed past decades. Almost papers discussed properties before and after radiation but images during radiation were not described yet. We have developed a new type of rad-hard pixel and integrated to 1.3M-pixel, 18-bit digital CMOS image sensor. Pixel area consists of several types of variation and the sensor has been analyzed during gamma ray radiation higher than 1 kGy/h up to 200 kGy. As the result, one type of pixel showed almost zero dark current increase at whole period.**

## I. INTRODUCTION

Radiation hardened CMOS image sensors (CIS) have been studied for more than past decade. An application of pinned photodiode (PPD) to 4-transistor (4T) pixel of CIS dramatically reduces dark current and it replaces charge-coupled devices (CCD) in high quality imaging applications. However, in radiation environment, PPD suffers deleterious impacts from irradiation and the dark current seriously increases [1-6].

After the accident at Fukushima Dai-ichi Nuclear Power Plant, there have been strong demand to monitor the nuclear plants continuously. It has already been developed high radiation hardened CMOS image sensors. In those cases, photo-sensitive areas were photodiode with field plate (FP-PD) [7-10] or pinned photo-gate (PPG) [11] structure. But even though such imagers are radiation hard, they show dark current increase along with total ionizing dose (TID). And past researches have focused on detecting the difference between before and after the irradiation [6-9]. It has been strongly requested to monitor the scenes of high radiation environment in real time.

In this paper, we discuss the images during gamma ray radiation higher than 1 kGy/h for newly developed pixels which were incorporated in 1.3M-pixel digital CMOS image sensors.

## II. DEVICE STRUCTURE

Fig. 1 shows block diagram of a newly developed CMOS image sensor. The sensor consists of pixel array, driving circuits and readout chain. All pixels are new type and pixel array consists of 3 parts; 1.3-M main pixels and 2 types of variations. Readout circuits are composed of analog CDS circuit, folding integration (FI) cyclic ADC [12], and digital readout circuits. FI samples 64 times and cyclic ADC is 12 bits, hence total ADC is 18 bits. Here, driving and readout circuits are not radiation-hardened-by-design (RHBD).

Fig. 2 shows device structure of the new pixel. Plan view is similar to pinned photogate (PPG) [11] but channel structure is different. In the case of PPG, silicon surface below the photogate is N- layer and photogate voltage (PG) is set to negative to introduce hole pinning layer. In the case of the new pixel, silicon surface is covered with P layer over the N- layer. Therefore, silicon surface can be accumulated by holes even for PG is positive. This brings reduction of electric field at the corner of charge detection N+ region adjacent to PG. We call the new pixel as PN photogate (PNPG).

Fig. 3 shows schematic potential profile of PPG and PNPG for depth direction. In the case of PPG, PG voltage need to be negative to introduce hole pinning layer at the silicon surface. In the PNPG case, PG voltage can be positive to accumulate holes at the silicon surface.

The device shown in Fig. 1 has been manufactured by 180 nm CIS process.

## Ⅲ. MEASUREMENT RESULTS

To confirm the channel potential of PPG and PNPG, test patterns for them were measured. Fig. 4 shows the result. Pinning voltage of PPG (Vgo) and P layer accumulating voltage of PNPG (Vgco) well correspond with target value. As the PNPG structure adds P layer at the silicon surface on PPG structure, this introduce hole accumulation layer at the surface even the PG voltage is positive. Therefore, electric field of a signal detection N+ area at the PG edge can be reduced on the condition that the surface under PG is covered with holes.

Fig. 5 shows dark output histogram of PPG depending on PG voltage before irradiation. When PG approaches to pinning voltage from –1.2V, dark output

signals near the median decrease but low probability large output pixels dramatically increase. This is attributed to high electric field at the charge detection area adjacent to PG (refer to Fig. 2).

Fig. 6 shows comparison of the dark output histogram among PPG and PNPG (2 types) structures before irradiation. In addition to small electric field of the detection area in PNPG structure due to 0V of PG, silicon surface is covered with holes by P layer. This brings low dark current at all probability region.

Finally, Fig. 7 shows dark output transition in the imaging mode under continuous gamma ray irradiation for PPG, PNPG_1 and PNPG_2. PNPG_1 is main pixel and PNPG_2 is one type of variation (refer to Fig. 1). Those data were measured every hour. In this case, maximum TID was limited not by devices but by usable time of radiation facility. Readout circuits were not RHBD but we have evaluated the readout circuits were functional until around 300[kGy].

In all cases, background gamma ray signal is calculated by following equation,

$$S_{rad} = \frac{1}{qK} R_{rate} \rho V_{pix} T_{\mathrm{int}}$$

where, $S_{rad}$ is signal electrons generated by radiation per pixel [e-], $R_{rate}$ is radiation rate [Gy/hr], q is electronic charge [C], K is electron-hole (e-h) pair generation energy for Si [eV/e-h], ρ is density of Si [kg/cm$^3$], $V_{pix}$ is effective pixel volume to accumulate generated electrons [cm$^3$], and $T_{int}$ is integration time to accumulate electrons [hr]. Calculated electrons from the equation well coincides with the measured result (50[A.U.] in Fig. 7). Note that this gamma ray signal is not temporally and spatially constant but randomly varying. The reason is considered that each gamma photon generates many e-h pairs through photoelectric absorption and Compton scattering process [13]. As absorption depth of gamma photons are very large in silicon, only a small part of them generate e-h pairs in the surface area. If radiation rate is small, images are flickering but in the case of Fig. 7, noisy gray images were obtained.

In Fig. 7, PPG (and also FP-PD) shows early anomaly, that is unusual increase of dark current in the dose region less than 100 kGy. The reason of the anomaly is not revealed now but PNPG dissolves the anomaly. Moreover, the pixel with optimized P-layer under the PG (PNPG_2) shows almost zero dark current increase under continuous irradiation from 0 to around 200 kGy of TID. The sensitivity and the dynamic range of the PNPG_2 are almost the same as those of PNPG_1.

This characteristic of zero dark current increase is probably the first realization in the literature. Fig. 8 shows captured image of PNPG_1 and PNPG_2 under continuous irradiation of gamma rays after 200 kGy. It clearly be seen that the PNPG_2 region is much low dark current compared with PNPG_1 even though PNPG_1 also low dark current on radiation environment after 200 [kGy].

As the rad-hard pixel is almost accomplished, our next step will be to fix the weaker part of readout circuit and to apply countermeasure for it.

## REFERENCES


[1] P. R. Rao et al., “Degradation of spectral response and dark current of CMOS image sensors in deep-submicron technology due to g-irradiation,” 37th Solid State Device Research Conference, pp.370, 2007.

[2] M. Innocent, “A radiation tolerant 4T pixel for space application”, in Proc. IISW, 2009

[3] V. Goiffon et al., “Radiation damages in CMOS image sensors: Testing and hardening challenges brout by deep sub-micrometer CIS process,” Proc. SPIE vol. 7826, 2010.

[4] X. Wang et al., “Design and characterization of radiation tolerant CMOS image sensor for space application,” Proc. SPIE, vol. 8194, 2011.

[5] J. Tan et al., “Analyzing the radiation degradation of 4-transistor deep submicron technology CMOS image sensors,” IEEE Sensors J., vol.12, pp.2278-2286, 2012.

[6] V. Goiffon et al., “Radiation effects in pinned photodiode CMOS image sensors: pixel performance degradation due to total ionizing dose,” IEEE Trans. Nucl. Sci., vol. 59, no. 6, pp. 2485–2491, Dec. 2012.

[7] B. Pain et al., “Hardening CMOS imagers: radhard-by-design or radhard-by-foundry,” Proc. SPIE vol. 5167, 2004.

[8] V. Goiffon et al., "Toward multi-MGy / Grad radiation hardened CMOS image sensors for nuclear applications," IEEE Trans. Nucl. Sci., vol. 62, no. 6, pp. 2956–2964, Dec. 2015.

[9] V. Goiffon et al., "Radiation hardening of digital color CMOS camera-on-chip building blocks for multi-MGy total ionizing dose environments,” IEEE Trans. Nucl. Sci., vol. 64, no. 1, pp. 45–53, Jan. 2017.

[10] V. Goiffon et al., "Challenges in improving the performances of radiation hard CMOS image sensors for gigarad (Grad) total ionizing dose,” in Proc. IISW, 2017

[11] T. Watanabe et al., "A new radiation hardeded CMOS image sensor for nuclear plant,” in Proc. IISW, 2017

[12] M-W. Seo et al., “A low-noise high-dynamic-range 17-b 1.3-Megapixel 30-fps CMOS image sensor with column parallel two-stage folding-integration/cyclic ADC”, IEEE Trans. Electron Devices, vol.59, pp.3396-3400, 2012

[13] G. Nelson and D. Reilly, “Gamma-ray interactions with matter,” http://faculty.washington.edu/agarcia3/phys575/Week2/Gamma%20ray%20interactions.pdf

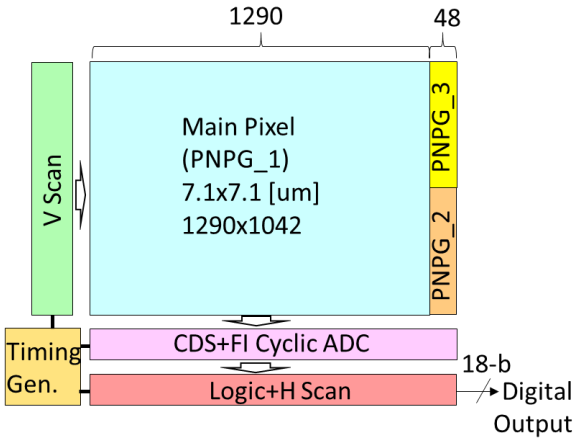


Fig. 1. Image sensor block diagram.

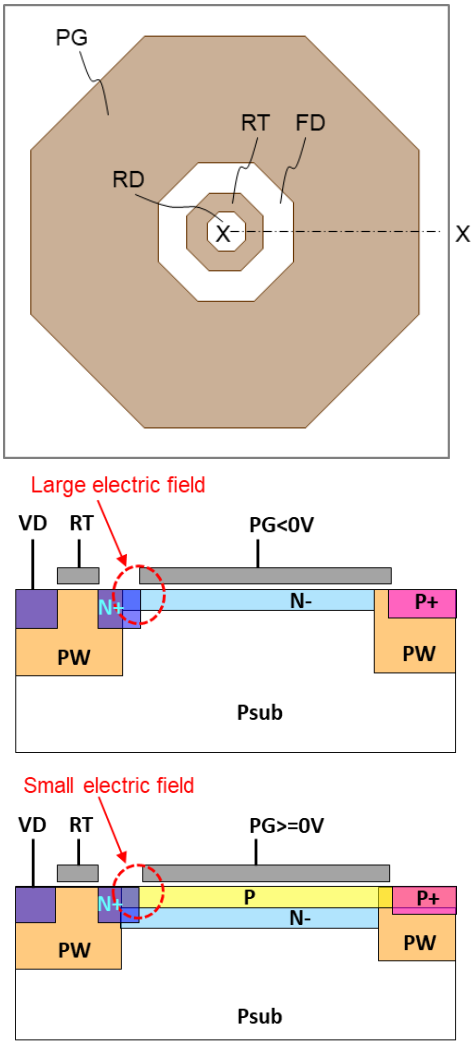


Fig. 2. Plan view of the pixel (top) and X-X line cross-sectional view of Pinned Photo-Gate (PPG) (middle) and PN Photo-Gate (PNPG) (bottom) structures.

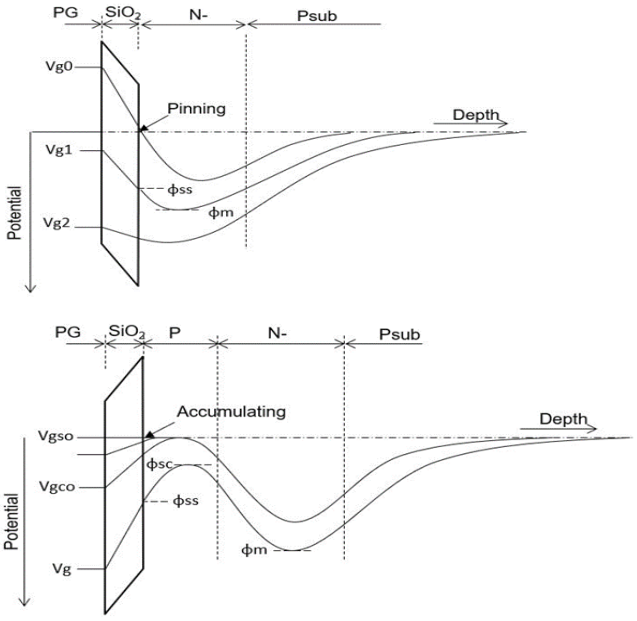


Fig. 3. Schematic potential profile of the PPG (top) and PNPG (bottom) for depth direction.

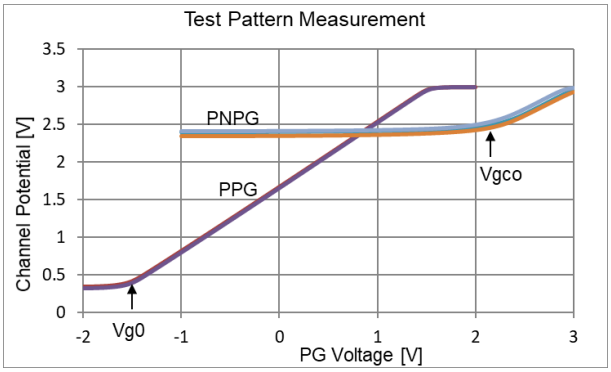


Fig. 4. Measured channel potential of the PPG and PNPG test patterns as a function of photo-gate (PG) voltage.

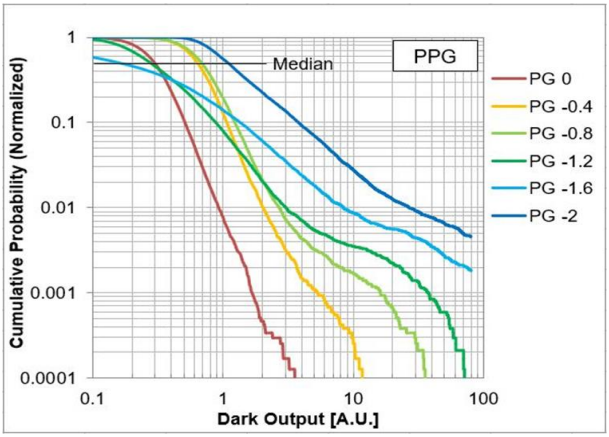


Fig.5. Dark output histogram of PPG before irradiation. PG was varied from 0V to -2V with 0.4V step.

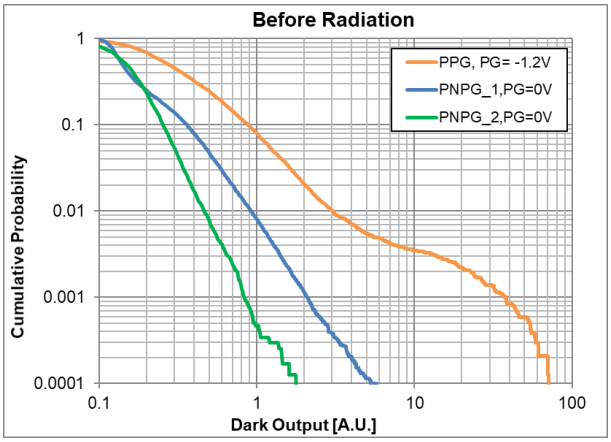


Fig. 6. Comparison of dark output histogram among PPG, PNPG_1 and PNPG_2 before irradiation.

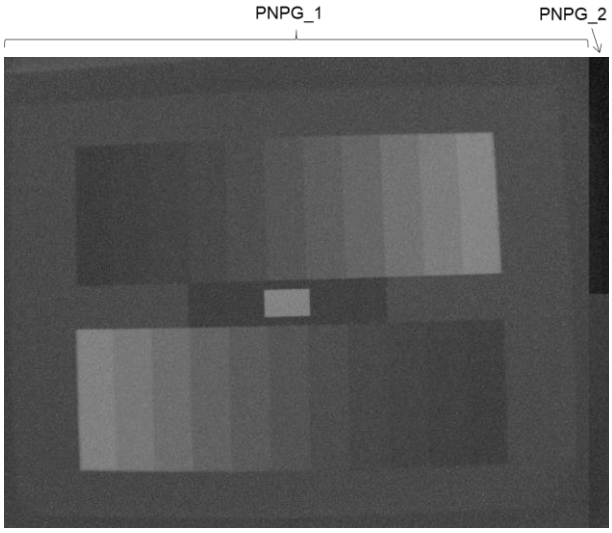


Fig. 8. Captured image of PNPG_1 and PNPG_2 under continuous irradiation of gamma rays after 200 kGy.

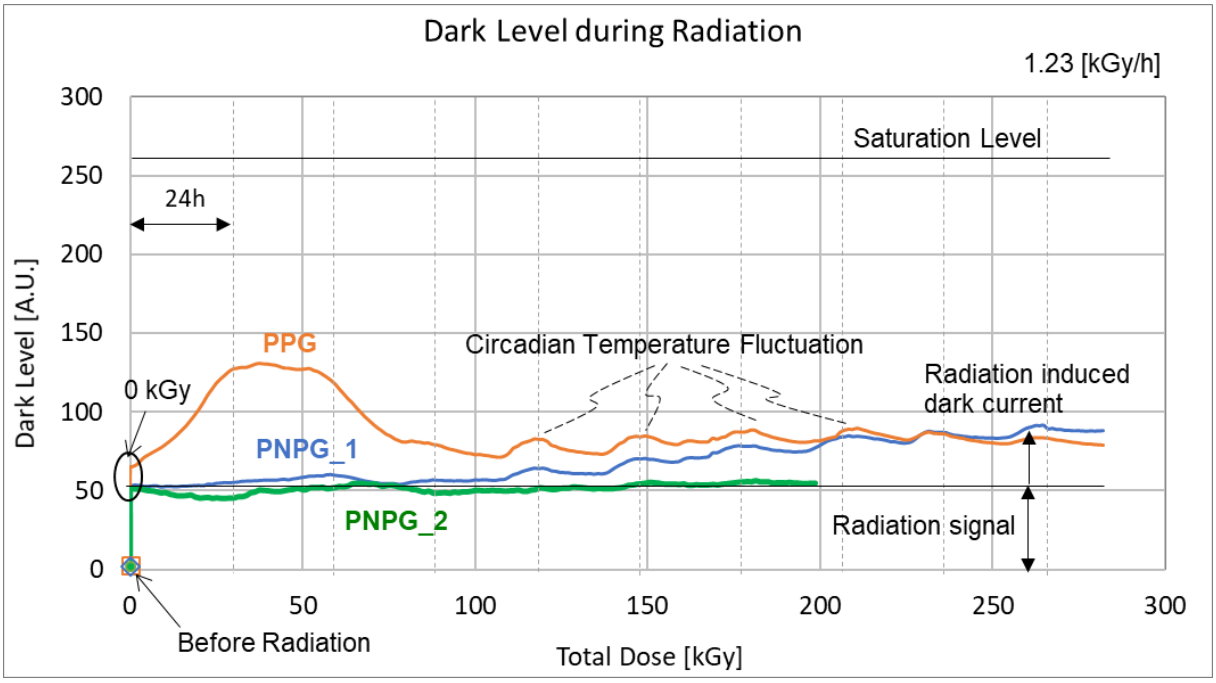


Fig. 7. Dark output level transition of three types of the pixel; PPG, PNPG_1 and PNPG_2 under continuous irradiation of Co60 gamma rays.

ACKNOWLEDGMENT

The project is supported by R&D program for Plant Safety Enhancement of the Agency for Natural Resources and Energy, Ministry of Economy, Trade and Industry (METI), Japan.